Taylor & Francis
Taylor & Francis Group

🔓 OPEN ACCESS Check for updates

High fidelity mini-LED backlit liquid crystal displays

Yuge Huang and Shin-Tson Wu

College of Optics and Photonics, University of Central Florida, Orlando, FL, USA

ABSTRACT
Mini-LED backlit liquid crystal display (LCD) exhibits premium display performance, benefiting from the new design space enabled by the mini-LED backlight unit: the flexibility in subframe sequential illumination enables motion blur reduction; the selective illumination of bright zones and dark zones offers high dynamic range, good sunlight readability and power saving; the high zone density suppresses the visual artefact of 'halo effect' that is commonly observed in conventional local dimming LCDs. In this paper, we discuss limiting factors and solutions to achieve high display fidelity regarding the abovementioned performance metrics.

Introduction

Information display brings much convenience to human life and has become an essential part of daily experience, thanks to the invention and development of display hardware technologies. Liquid crystal display (LCD) technology evolved several times in the past half century: from the original discovery of dynamic scattering effect to the identification of twisted nematic field effect for mass applicable LCD [1–5], followed by the vertical alignment mode and the fringe-field switching mode for enhanced contrast ratio and wide viewing angle [6,7], nowadays LCD has proven its success and reliability. Meanwhile, organic light-emitting diode (OLED) display technology grows rapidly, thanks to the extensive efforts on materials and devices [8–10]. OLED display offers excellent dark state, thin profile and flexible options, making it gradually leads on small panels such as smartphones and smartwatches. In parallel, electronic paper displays feature print-like visual experience and low power consumption, making it especially favourable for E-books and public displays [11–13]. On the other hand, micro-LED display is emerging and bears expectations of high brightness, long lifetime and compact package [14–19]. Recently, the boom of computation technology enables the generation and process of explosively larger volume of information; reflected on the rich media contents, it calls for an upgrade on the information display hardware. Performancewise, the end target is to mitigate the difference between the natural scene and the displayed image with respect to the metrics of luminance, static resolution, dynamic sharpness and colour.

Conveniencewise, consumers favour devices with light weight, slim profile and long battery life that work robustly in various environments.

Traditional LCD is limited by several performance trade-offs. First, the non-ideal alignment and the scattering effect on the LC layer and the colour filter restrict the LCD contrast ratio to 5000:1 [20,21]. As a result, the display is not able to present both the dark details and the highlight contents in a single image. Second, suppose the LCD has a very high contrast ratio as we need, the optical efficiency remains low in comparison with emissive displays. The power consumption of a traditional LCD is determined by the peak luminance; the backlight consumes the full electrical power to illuminate all pixels to the peak luminance, and the LCD panel cuts off the transmittance of each pixel according to the image content. This non-emissive display mechanism asks designers to make a choice: a relatively dim backlight for low power consumption with compromised sunlight readability, or a very bright backlight at the price of high power consumption [22]. Third, both high spatial resolution and high refresh rate demand more budget on driving time, which is especially tight to satisfy today's needs: the pixel count of 4K2K (8K4K) and the refresh rate of 144 (240) frames per second (fps).

The mini-LED backlit LCD [18,23–26] could bring LCD technology to a new stage. Figure 1 is a schematic of the system configuration, including an LCD panel for pixel-by-pixel intensity modulation and a mini-LED backlight unit (mLED BLU) for two-dimensional (2D) arrayed direct-lit local dimming [22,23,27]. The LCD panel
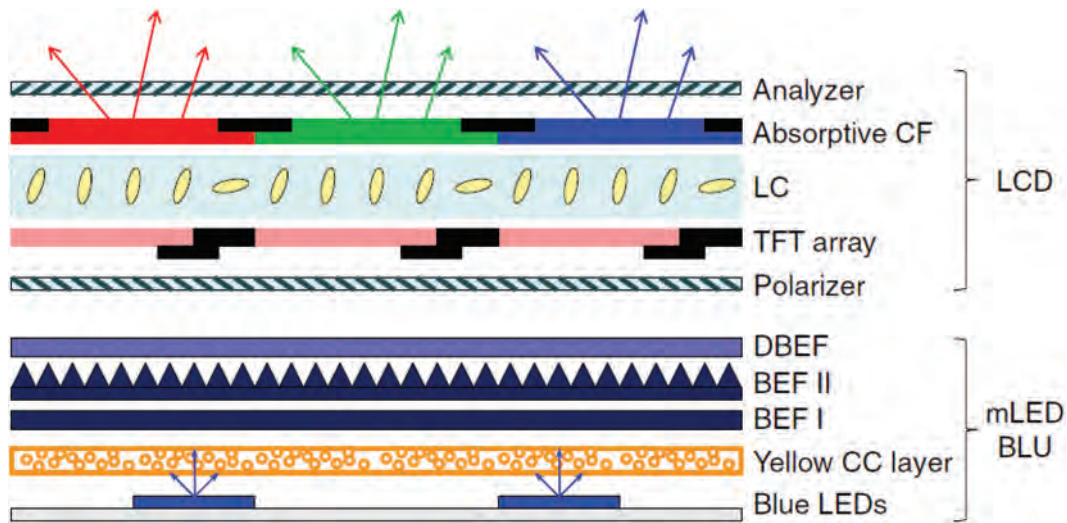
Figure 1. The system configuration of a mini-LED backlit LCD. Reproduced from Ref. [18], with the permission of Springer Nature.

contains an LC layer sandwiched between crossed polarisers, which responds to the electric field and modulate the polarisation rotation and the output intensity. A full-colour pixel includes three subpixels; the colour of each subpixel is determined by the RGB colour filter (CF); the luminance transmittance of each subpixel is determined by the voltage signal given by a thin film transistor (TFT). The mini-LED BLU typically uses blue LED chips because of the higher quantum efficiency than the red and the green. A portion of the blue light pumps the quantum dots or the phosphors in the yellow colour conversion (CC) layer to generate yellow (or red plus green) light, and mixes with the unconverted blue light for a white colour [28,29]. Two brightness enhancement films (BEFs) collimate the wide-angle emission into the ± 30° angular cone of interest in two in-plane directions. Without intentional asymmetric designs, the light from LEDs and colour converters are normally unpolarised. As a result, no more than half of the light can transmit the LCD polariser. To increase the transmission efficiency, a dual brightness enhancement film (DBEF) recycles the light in the undesired polarisation into the preferred polarisation [30].

Mini-LED BLUs are especially designed for local dimming functionality [22,23,27]. The BLU is divided into a 2D zone array; each zone can be turned on and off independently and each zone contains multiple mini-LED units. For illustration purposes, we only draw one full-colour pixel in the LCD part and two mini-LED units in the mLED BLU part in Figure 1. In real display systems, each mini-LED zone illuminates multiple full-colour pixels. In the following sections, we discuss how such 2D-arrayed BLU improves the display performance providing the additional degrees of freedom in the design space. We develop new driving schemes, fast response LC materials and conducted performance-driven analysis to optimise the display system structures. Specifically, we use the following performance metrics to describe the enhancement: motion blur [31,32], dynamic range [33–35], sunlight readability [18,25,36,37] and power consumption [18].

Motion blur and display response time

Motion blur is an artefact commonly observed on fast-moving objects. Because the displayed image is refreshed frame by frame, the displayed object moves in a step-by-step behaviour instead of the natural continuous translation. This inconsistency results in a blurry image in perception. Figure 2(a) shows a static displayed project with a sharp profile. However, when the object moves fast horizontally, the same displayed project is perceived blurry along the moving direction, as shown in Figure 2(b). Motion blur can be reduced by decreasing the image persistence time on the screen in three ways: 1) increasing the frame rate, 2) decreasing the backlight duty ratio, and 3) employing fast response LC materials and modes.

High frame rate

Increasing the display frame rate (*f*) can shorten the image persistence time, which equals to the frame time ($T_f = 1/f$) if the backlight duty ratio is 100%. As shown in Figure 3, the perceived image quality is noticeably improved as the frame rate increases from 60 fps to 180 fps and saturates at higher frame rates. The perceived image quality was

Figure 2. Illustration of motion blur. (a) Original profile of the displayed object. (b) Perceived blurry profile when the object is moving with a high speed in display. Reproduced from Ref. [38], with the permission of the author.
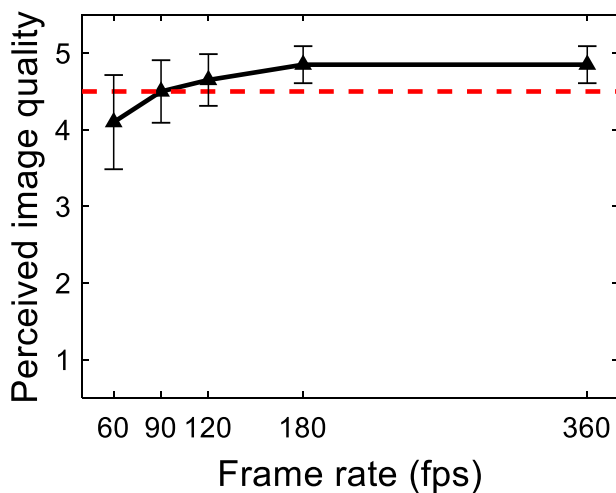

Figure 3. Perceived image quality at different display frame rates. The rating grade '1' to '5' corresponds to 'completely different', 'very different', 'different', 'slightly different' and 'identical', respectively.

obtained by averaging subjective ratings of the sharpness difference between a static displayed object and a fast-moving displayed object at a 24°-per-second angular speed, which corresponds to the perceived sharpness difference between Figure 2(a,b). The higher perceived image quality, the less difference is perceived.

Low backlight duty ratio

Low backlight duty ratio reduces motion blur as well, which can be analysed case by case according to the display type and the driving scheme. Figure 4(a) illustrates the emission pattern of a conventional active matrix LCD, where the horizontal axis is time and the vertical axis is a spatial direction in the panel plane. Two frames are drawn here for illustration purposes. In the drawing, we fully filled the background with a light
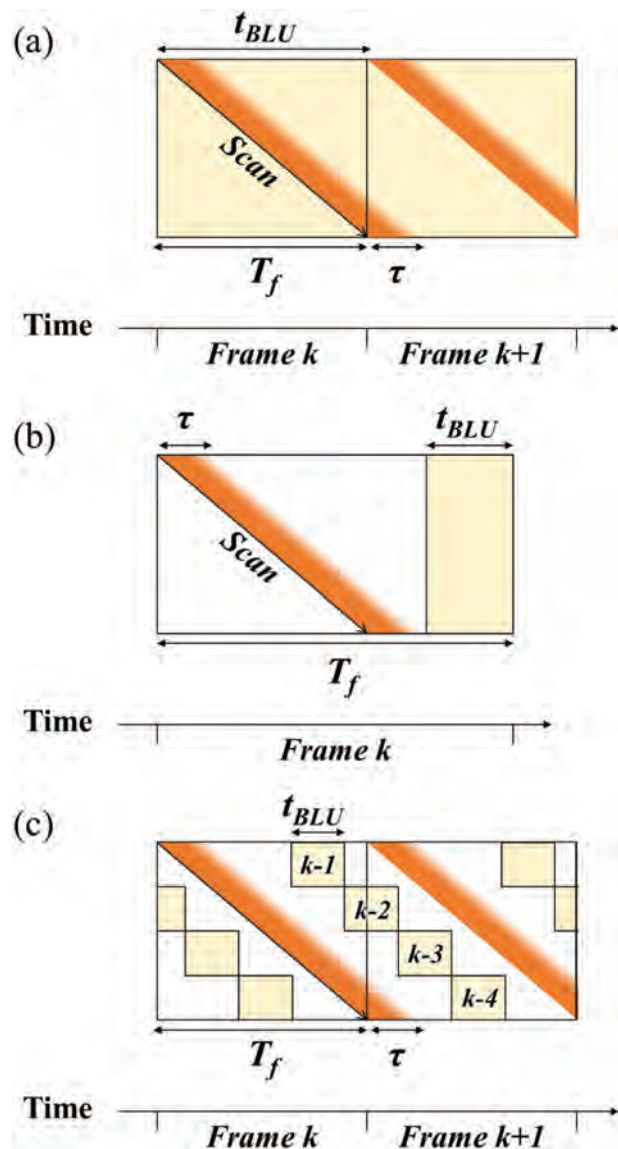

Figure 4. Active matrix LCD emission patterns: (a) continuous progressive emission, (b) simultaneous emission and (c) segmented progressive emission.

orange shade to imply that the backlight has a duty ratio of 100%, which makes the backlight-on time in each frame equal to the frame time ($t_{BLU} = T_f$). Throughout each frame, the gate transistor of each row opens sequentially to send the image update signal row by row from the top to the bottom of the panel. In Figure 4(a), the gate opening time of *Frame k* is delineated by the diagonal black line 'Scan'. The dark orange shade following the 'Scan' line shows that it needs an LC response time (τ) to complete the LC transition from the previous image to the new image after the signal is updated. In such a continuous progressive driving scheme, the image persistence can be described by motion picture response time (MPRT) [31], which is simplified as [32]

$$MPRT = \sqrt{\tau^2 + (0.8T_f)^2}. \tag{1}$$

When $\tau << T_f$, Equation (1) shows that a conventional active matrix LCD's MPRT is mainly determined by the frame time, which can also be observed in Figure 5.

Practically, frame rate cannot be infinitely high because scanning speed is limited and higher frame rate means higher power consumption. To walk around the challenge of an ultrahigh frame rate, simultaneous emission pattern with low duty ratio is adopted to reduce MPRT. As illustrated in Figure 4(b), the row-by-row scanning process and the LC transition are completed within partial frame time; leaving a dedicated time window for backlight illumination and image persistence, as denoted by the light orange shade in Figure 4(b). Using this simultaneous emission pattern, the motion picture response time is reduced to
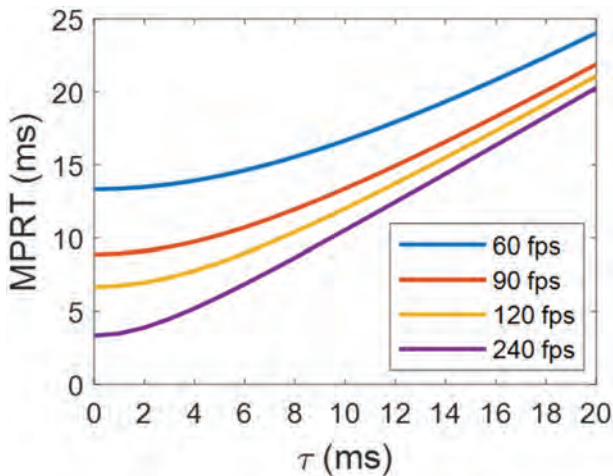
$$MPRT = 0.8t_{BLU} = 0.8T_f \cdot DR. \tag{2}$$

Figure 5. Motion picture response time as a function of LC response time (τ) and frame rate. Reproduced from Ref. [18], with the permission of Springer Nature.

Equation (2) gives an encouraging message that a 10% duty ratio (DR) can bring a benefit of 10 times faster MPRT which otherwise requires 10 times higher frame rate. However, a side effect of this solution is that low duty ratio demands high instant brightness boost. For example, a 10% duty ratio requires 10 times higher instant brightness in the backlight-on window to obtain the same perceived brightness after the time average effect. Such a brightness boost could force the backlight LEDs to operate at a unfavourable high current and low efficiency region.

Segmented emission pattern is capable of achieving intermediate duty ratio and fast MPRT at the same time. As shown in Figure 4(c), the segmented backlight zones are turned on sequentially following the scanning process and the LC transition. Four zones turned on at four time blocks are drawn in Figure 4(c) for *Frame k* as 'k-1' to 'k-4'. The image content in each zone needs to be adjusted at subframe level to obtain the fast MPRT calculated by Equation (2). It is worth mentioning that a zonal BLU is necessary for such a segmented emission pattern, and mini-LED BLU is a good candidate. The three driving schemes shown in Figure 4 also apply to micro-LED/OLED emissive displays if the LCD response time (τ) is replaced by the LED response time, which is at nanosecond level for Micro-LEDs and microsecond level for OLEDs.

Fast response LC materials and modes

Fast LC response time can reduce MPRT. According to Equation (1) and Figure 5, when $\tau << T_f$ in continuous progressive emission pattern, further reducing LC response time makes little improvement on MRPT. According to Equation (2) and Figure 4(b,c), when LC response time is not a limiting factor of duty ratio and frame rate in simultaneous emission pattern and segmented progressive emission pattern, it no longer drags MPRT. For the goal of making the MRPT of LCD to a level comparable to that of a micro-LED/OLED display, the target of LC response time is $\tau < 2$ ms and preferably $\tau < 1$ ms. Such a fast LC response time can be achieved by developing LC materials, LC cell structures and driving circuitry. For practical panel applications, we monitored other specs such as work temperature, driving voltage and photostability as well.

The LC response time is determined by material properties, including viscosity (γ_1), elastic constants (K_{11}, K_{22} and/or K_{33} for anti-parallel alignment, twisted nematic alignment and vertical alignment, respectively) and cell gap (d) [39,40]:

$$\tau_{LC} \propto \frac{\gamma_1 d^2}{K_{ii}\pi^2}. \tag{3}$$

Low viscosity contributes to fast LC response time. However, such materials typically have low birefringence

(Δn) and/or low dielectric anisotropy ($\Delta\varepsilon$), which requires a thicker cell gap to fully flip the polarisation by π phase modulation. As a result, the thick cell gap in return slows down the response time. On the other hand, a large elastic constant helps reduce LC response time, making the use of the large K_{33} (typically > K_{11} > K_{22}) favourable. However, the negative LC material ($\Delta\varepsilon < 0$) has a smaller candidate pool, and it frequently suffers from the trade-off between large dielectric anisotropy ($|\Delta\varepsilon|$) and low viscosity (γ_1). It is importantly to develop LC materials with balanced properties, including low viscosity (γ_1), large dielectric anisotropy ($|\Delta\varepsilon|$) and high birefringence (Δn).

Because of the square relationship between τ and d, we adopted a thin-cell strategy and optimised LC materials for high birefringence [41]. Table 1 shows the grey-to-grey response time of an optimised LC material in a 90° mixed-mode twist nematic (MTN) cell with d = 1.32 μm. We sampled the switching transition between five grey levels (GL = 0, 64, 128, 192 and 255) found by the transmittance $T = (GL/255)^{2.2}$. In addition to the 0.9-ms average grey-to-grey response time, this material exhibits favourable physical properties for the application in the liquid-crystal-on-silicon (LCoS) panel for augmented reality displays, including a wide nematic temperature range (−40 ~ 86.5°C), high birefringence (Δn = 0.251 at 550 nm), high dielectric anisotropy ($\Delta\varepsilon$ = 6.68 at 1 kHz), low viscosity (γ_1 = 133 mPa·s at 25°C) as well as the required resistivity and photostability.

In addition, the LC response time can be reduced by adding confinement in more dimensions. Mainstream LCD modes are 1D confined: the restoring force is provided by the two substrates and the distance in between is the cell gap. Researchers also proposed 2D confinement structures: by introducing a symmetric design of the electrode and the alignment, 'virtual walls' are self-formed during electrical switching and provides additional restoring force to accelerate the response [42–44]. This method effectively enhances response time by two times. The drawback of such design is the reduced transmittance. Because the 'virtual wall' region does not respond to electric fields, it forms a dead zone and reduces the LCD active aperture. Faster response time needs denser virtual walls and leads to lower transmittance.

Moreover, polymer-stabilised LC offers much smaller 'd' in Equation (3). Polymer-stabilised LC precursors contain reactive mesogen compounds that can be polymerised by UV light. The formed polymer network functions as in-cell body alignment structures that restore LC molecules from the deformation under electric field to the initial alignment. As a result, the 'd' in Equation (3) is determined by the polymer network structural size which is smaller than the cell gap. The polymer network can also be considered as 'walls', and the goodness is it does not decrease active aperture. Polymer-stabilised blue-phase liquid crystal (PSBPLC) [45,46] and polymer network liquid crystal (PNLC) [47–49] are fast-response solutions for displays at visible wavelength and phase modulators at infrared wavelength, respectively. For displays at visible wavelength, PSBPLC offers attractive features for LCD such as sub-millisecond response time and optically isotropic dark state, as well as the fabrication convenience of no surface alignment and high tolerance on the in-plane switching (IPS) cell thickness. The biggest challenge of the commercial use of PSBPLC in displays is the high operation voltage. To lower the voltage, researchers developed LC materials with ultrahigh dielectric anisotropy [50–52], whereas some other properties are compromised: (1) the increased viscosity slows down the response time; (2) the ultrahigh dielectric constants lead to slow capacitor charging time and high power consumption. Additionally, a protruded electrode structure was proposed to reduce the operation voltage by activating a thicker LC layer [53,54]. A small protrusion area make a small dead zone and increase the transmittance, whereas when the aspect ratio of the protrusion is too high, it leads to low yield and high cost in manufacturing. A practical design is to balance the material properties of dielectric constants and viscosity, control the polymer network domain size, and employ a protruded electrodes with a moderate aspect ratio. A blue-phase LC precursor JC-BP08 was optimized using this strategy [55]. After polymer stabilization, the material (PSBP-08) exhibits submillisecond response

Table 1. Measured grey-to-grey response time of an optimized LC material in a 90° mixed-mode twist nematic (MTN) cell.

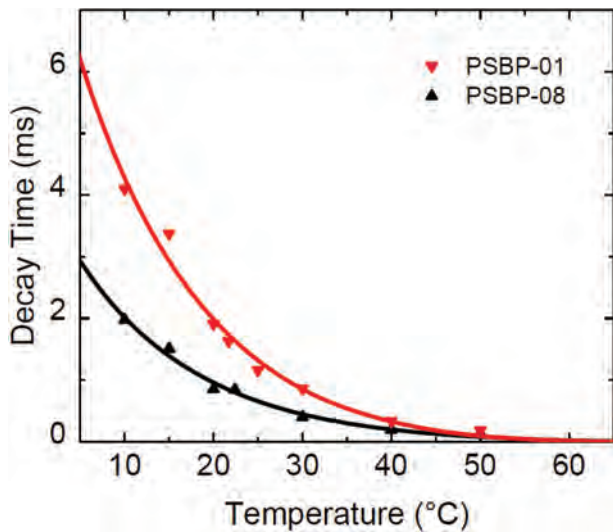| Decay time (ms)	GL	Rise time (ms)				
		255	192	128	64	0
	255	*	2.401	1.363	0.648	0.136
	192	0.781	*	1.339	0.517	0.110
	128	0.762	1.916	*	0.493	0.123
	64	0.731	1.743	1.078	*	0.260
	0	0.698	1.619	0.825	0.476	*

Reproduced from Ref. [41], with the permission of Optica.

Figure 6. Temperature-dependent decay time of PSBP-01 and PSBP-08 at λ = 633 nm and frame rate = 240 Hz. Dots are experimental data and lines are fitting curves. Reproduced from Ref. [55], with the permission of Optica Publishing Group.

time at room temperature or higher temperature, as plotted in Figure 6. Applying the triangular protrusion electrode structure [56], it enables single-TFT driving (15 V) for 74% transmittance and a charging speed (~250 µs) manageable with pre-charging methods.

High dynamic range

High dynamic range (HDR) display aims to faithfully reproduce images with high luminance range and wide colour gamut [34,35,57]. True-to-life colour reproduction can be realised by engineering the R/G/B light source to cover the Rec. 2020 colour gamut, which requires proper central wavelength (ideally 630 nm, 532 nm and 467 nm) and narrow bandwidth [57]. Specifically, wide colour gamut LCD (>95% Rec. 2020) can be made by employing proper LEDs, quantum dots, perovskite and narrowband colour filters [28,29,58,59]. On the other hand, high luminance range and high bit depth are unique features of mini-LED backlight LCD, which is the main focus of this section.

HDR requires a luminance range of 0.005 ~ 10,000 cd/m^2 and 12-bit grey levels to produce nature-like images [35]. As a reference, conventional LCDs exhibit <5000:1 contrast ratio and 8-bit grey levels. Local dimming technology can significantly improve LCD contrast ratio by selectively turn on the backlight array [22,23,25]. Whereas halo effect and clipping effect degrade the image quality on local dimming LCDs [60,61]. Halo effect is the over-illumination of the dark area surrounding brighter objects, which can be observed as the whitish 'halo' around the flowers in Figure 7(b) in comparison to the original image in Figure 7(a). Reversely, clipping effect is the insufficient illumination of the bright object surrounded by dimmed regions. Both halo effect and clipping effect can be managed by optimising the backlight design and the LCD panel contrast ratio.

Mini-LED backlit LCD

Mini-LED backlight offers high local dimming zone density and fine control on the spatial and angular illumination uniformity. Taking Figure 8 as an example, to display the candle image in Figure 8(c), the white backlight is turned on in a zonal manner according to the brightness need in each zone. Here, each zone contains 6 × 6 mini-LEDs as represented by the white dots in Figure 8(a). After the colour conversion layer and the diffuser, the luminance within each local dimming zone becomes uniform, as shown in Figure 8(b), before the full-colour LCD modulation to generate the image in Figure 8(c).

Several aspects determine the performance of a local dimming LCD. First, the contrast ratio within each local dimming zone is limited by the LCD model. For example, twisted-nematic (TN) mode [2], fringe-field switching (FFS) mode [7] and multi-domain vertical alignment (MVA) mode [6] respectively gives a contrast ratio of ~1000:1, ~2000:1 and ~5000:1. Second, the display luminance uniformity and the inter-zone crosstalk are determined by the backlight illumination profile [25]. Well-confined illumination within each zone reduces the inter-zone crosstalk, but the sharp change between adjacent zones leaves little tolerance on fabrication registration and makes the zone border more
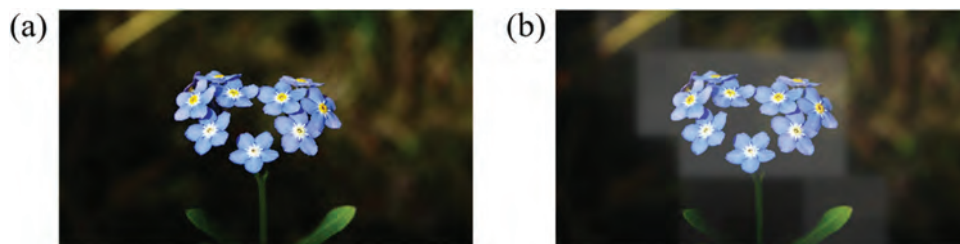

Figure 7. (a) Target image. (b) Local dimming displayed image with halo effect around the bright object. Reproduced from Ref. [38], with the permission of the author.
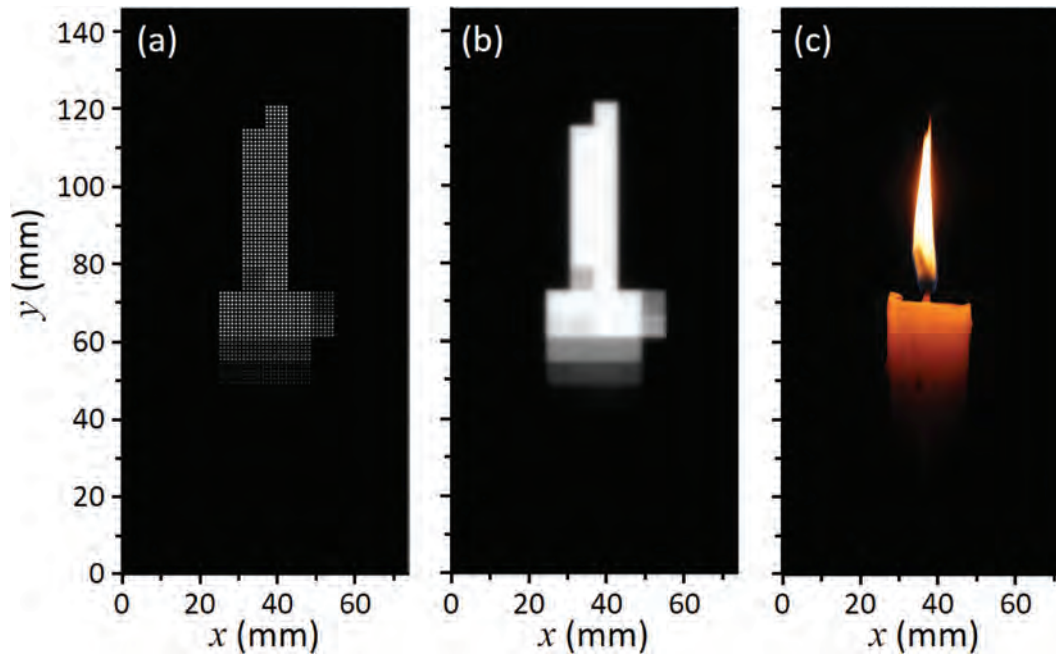
Figure 8. Displayed image simulation: (a) mini-LED backlight modulation; (b) luminance distribution of the light incident on LC layer, and (c) displayed image after LCD modulation. Reproduced from Ref. [23], with the permission of Optica Publishing group.

noticeable. Third, appropriate local dimming algorithm can improve the image reproduction accuracy and reduce power consumption [60]. Fourth, the local dimming zone density is critical [23,25]. The lesser local dimming zones, the more obvious halo effect. On the contrary, dense local dimming zones means a large number of small-size LED chips. In addition to the increased fabrication cost and the increase driving power to independently control these zones, the side-wall loss on small-size LEDs makes their quantum efficiency lower than large-size LEDs (>50 µm) [62].

In order to identify appropriate density of local dimming zones, we conducted optical simulations and subjective experiments, and found the optimal density depends on the LCD panel contrast ratio, the panel size and the viewing distance [23]. We used the peak signal-to-noise ratio in LAB colour space (LabPSNR) to describe the difference between a displayed image on a mini-LED backlit LCD and the target image. Subjective experiments show that LabPSNR >47.4 dB is the bar where > 95% observers cannot tell the difference. The simulated LabPSNR on different mini-LED backlit LCD systems are plotted in Figure 9, where the panel size is 6.4 inch and the viewing distance is 25 cm. As expected, more local dimming zones leads to higher LabPSNR, indicating higher display fidelity. To reach the bar of LabPSNR >47.4 dB, the backlight needs ∼ 200 independent dimming zones for LCD contrast ratio = 5000:1, and ∼ 3000 zones for LCD contrast ratio = 2000:1. If the LCD contrast ratio is as low as 1000:1, halo effect remains noticeable
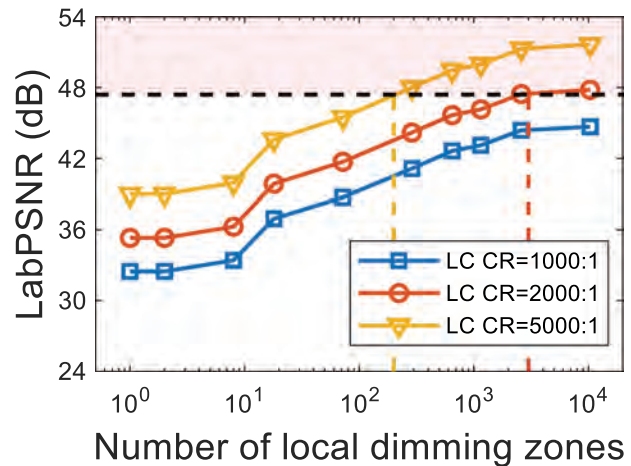

Figure 9. Simulated LabPSNR for different HDR display systems with various local dimming zone numbers and LC contrast ratios. Reproduced from Ref. [23], with the permission of Optica Publishing Group.

even with >10000 zones, which means higher LCD contrast ratio and more local dimming zones are needed. The study results can be applied to universal panel size and viewing distance by designing the local dimming backlight to meet the critical angular zone density to be ∼ 0.61 zones per degree, ∼2.35 zones per degree, and > 6.06 zones per degree for the LC contrast ratio of 5000:1, 2000:1 and 1000:1, respectively. These angular density values can be converted to zone size as well, such as the need of a 2-mm zone pitch for a FFS smartphone and a 58-mm zone pitch for a MVA TV, as listed in Table 2.

Table 2. Exemplary calculation of required local dimming zone density on applications using different LC modes: twisted-nematic (TN) mode, fringe-field switching (FFS) mode and multi-domain vertical alignment (MVA) mode.

Application	LCD contrast ratio	Viewing distance	Zone pitch
Notebook	1000:1 (TN)	50 cm	2 mm is insufficient
Smartphone	2000:1 (FFS)	25 cm	2 mm
TV	5000:1 (MVA)	2 m	58 mm

While the above discussion assumed a square lattice layout where mini-LEDs are periodically places along two orthogonal directions in the plane, other layouts are developed such as Apple's dithered layout combining a square lattice and a hexagon lattice for minimising grid mura perception [26]. The required pitch density needs to be adjusted with the mini-LED layout and emission profile accordingly.

Power consumption and sunlight readability

Power consumption

The power consumption of a mini-LED backlit LCD is on the backlight illumination and the backplane driving circuits [18,63,64]. For high-brightness and large-size panels, the LEDs in the backlight consume most of the power. Let's start with the blue mini-LED chips and go through the backlight power calculation using the system described in Figure 1. The LED efficacy (η_{LED} [unit: lm/W]) is the ratio of the emitted luminous flux Φ ([unit: lm]) to the consumed electrical power P_{LED} ([unit: W]):

$$\eta_{LED} = \frac{\Phi}{P_{LED}} = \frac{K \cdot E_{ph}}{e} \cdot \frac{EQE_{LED}}{V_F}. \tag{4}$$

Here K is the luminous efficacy, E_{ph} is the photon energy, e is the elementary charge, EQE_{LED} is the blue mini-LED's external quantum efficiency (EQE), and V_F is the LED forward voltage. The colour conversion layer converts partial blue light to yellow (or red and green) with an efficiency EQE_{CC}. Two BEF layers and one DBEF layer, respectively, collimate the light and recycles the undesired polarisation, corresponding to a conversion coefficient F as the ratio of luminous flux Φ [unit: lm] to on-axis luminous intensity [unit: cd]. The luminous transmission on the optical films in the backlight unit is estimated as T_{BLU} including loss caused by index mismatch and absorption. The LCD panel optical efficiency is simplified as T_{LCD} (typically ~0.05 for RGB colour filters and ~ 0.1 for RGBW colour filters). Therefore, the mini-LED backlit LCD system on-axis luminous power efficacy (η_{sys} [unit: cd/W]) for colour j = R, G, B can be expressed as

$$\eta_{sys,j} = \eta_{LED} \cdot \frac{EQE_{CC,j} \cdot T_{BLU} \cdot T_{LCD}}{F_j}. \tag{5}$$

By introducing colour mixing ratio r_j to mix R, G and B into white colour, the on-axis luminous power efficacy for white light ($\eta_{sys,W}$ [unit: cd/W]) is

$$\eta_{sys,W} = \frac{1}{\sum_j \frac{r_j}{\eta_{sys,j}}}. \tag{6}$$

This calculation flow has been validated on a 1000-nit 65-inch 4K TV. Using the parameters in Table 3, the calculated backlight power consumption P_{LED} = 284 W agrees well with the measurement of 280 W.

Sunlight readability

Sunlight readability measures the outdoor performance of a display. High sunlight readability can be achieved by appropriate design of the display structure [18,25,37]. Figure 10 is an example showing the simulated perceived images produced with different display brightness in different ambient conditions. As the environment becomes brighter, the image is less and less recognisable. Unfortunately, sunlight readability is a frequent issue on vehicle displays; extracting navigation information from such images distracts drivers from focusing on road conditions and gives rise to safety concerns. The most straightforward method to increase sunlight readability is to increase display brightness, but the price is high power consumption and additional demands on heat dissipation. In the following, we show the quantitative method of evaluating sunlight readability vs. power consumption, and demonstrate mini-LED backlit

Table 3. Parameters to calculate the on-axis power efficacy of a mini-LED backlit LCD. Reproduced from ref [18], with the permission of Springer Nature.

Colour	Red	Green	Blue
K (lm/W)	186	526	84
E_{ph} (J)	3.1×10^{-19}	3.7×10^{-19}	4.3×10^{-19}
EQE_{LED}	–	–	0.5
V_F (V)	–	–	2.8
EQE_{CC} [65]	0.73	0.73	1
$EQE_{LED} \cdot EQE_{CC}$	0.37	0.37	0.5
T_{BLU}		0.9	
F (lm/cd) [30]		0.96	
T_{LCD}		0.05	
r	0.247	0.672	0.081
η_{sys} (cd/W)	2.2	7.4	1.9
$\eta_{sys,W}$ (cd/W)		4.1	
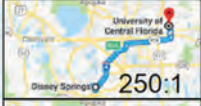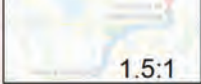
Figure 10. Simulated perceived images on displays with different peak luminance under various ambient conditions. The numbers at the right bottom corner of the images represent the ambient contrast ratio. Reproduced from Ref. [25], with the permission of John Wiley and Sons.

LCD's opportunity in comparison with other display methods.

In outdoor scenarios, the display reflection of strong ambient light impairs the information readability. Ambient contrast ratio (ACR) describes the perceived image contrast on a display panel. For the 'signal', the display peak luminance is much higher than the display dark state luminance ($L_{peak} >> L_{dark}$). For the 'noise', the ambient reflection forms a background that is determined by the ambient illuminance (I_{am}) and the luminous display reflection (R_L). Let's limit the discussion to the condition that the perceived image is readable (ACR >> 1). Therefore, ambient contrast ratio can be approximated as:

$$ACR = \frac{L_{peak} + \frac{I_{am}}{\pi} \cdot R_L}{L_{dark} + \frac{I_{am}}{\pi} \cdot R_L} \approx 1 + \frac{\pi \cdot L_{peak}}{I_{am} \cdot R_L} \approx \frac{\pi \cdot L_{peak}}{I_{am} \cdot R_L}. \quad (7)$$

Here L_{peak} can be substituted with the total LED power ($P_{panel,W}$), the panel size (A_{panel}) and the on-axis luminous power efficacy ($\eta_{sys,W}$) [38]:

$$ACR \approx \frac{\pi}{I_{am}} \cdot \frac{P_{panel,W}}{A_{panel}} \cdot \frac{\eta_{sys,W}}{R_L}. \quad (8)$$

Equation (8) helps us categorise the factors influencing ambient contrast ratio: in the first part, I_{am} reflects the display work environment; in the second part, $P_{panel,W}$ and A_{panel} are predetermined panel specifications; the third part $\eta_{sys,W}/R_L$ comes from design parameters, which can be considered as a figure of merit to optimise displays for high sunlight readability and low power consumption.

Equation (8) is universal for different display types, including micro-LED/OLED emissive displays, which enables us to compare the sunlight readability and power budget of different displays. From Equations (4)-(6), $\eta_{sys,W}$ is proportional to EQE_{LED}/V_F, making $\eta_{sys,W}$ very sensitive to the chip size of micro-LEDs while remaining stable for OLEDs and mini-LEDs. On the other hand, R_L is determined by the anti-reflection surface treatment (normally 2 ~ 4%) for mini-LED backlit LCDs, while for those OLED/micro-LED emissive displays without circular polariser (CP) lamination, it additionally depends on the LED chip aperture. For a fair comparison, we preset the target ambient contrast ratio in the typical work environment according to the application (smart phone, notebook and TV), and calculate the required LED power consumption of these displays. We used experimental data on micro-LEDs with various chip sizes [17,66,67], mini-LEDs with a fixed 200-µm chip size, and state-of-the-art OLEDs [68–71] in the calculation. The results are plotted in Figure 11 and show that each display technology has its own strength in certain region. RGB-chip micro-LEDs have a strong display reflection due to the bottom reflector, which makes it favourably to design a small LED aperture (shown as the blue solid lines) or a combination of a large LED aperture and a circular polariser (shown as the red solid lines). Mini-LED backlit LCDs (shown as the green dashed lines) and OLED displays (shown as the purple dashed lines) suit for small-pixel displays in brighter ambient conditions (shown by Figure 11(a)) rather than large-pixel TVs in dim environment [shown by Figure 11(c)].
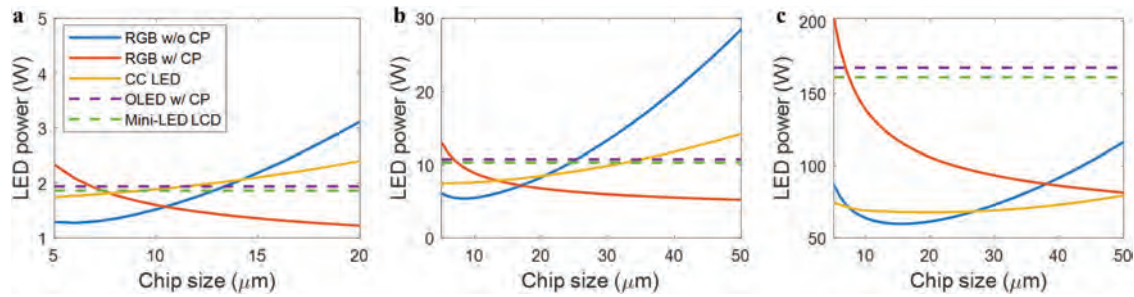
Figure 11. Chip size dependent LED power consumption with different display technologies: a RGB-chip emissive micro-LED display without circular polarizer (RGB w/o CP) and that with a circular polarizer (RGB w/CP), a color conversion emissive micro-LED display (CC LED), a RGB-chip emissive OLED display with a circular polarizer (OLED w/CP) and a mini-LED backlit LCD (mini-LED LCD). Application scenarios: (a) 50-μm pitch smartphone under 1500-lux overcast daylight for ACR = 40:1. (b) 90-μm pitch notebook under 500-lux office light for ACR = 100:1. (c) 375-μm pitch (65-inch 4K) TV under 150-lux living room ambient for ACR = 1000:1. Reproduced from Ref. [18], with the permission of Springer Nature.

Conclusion and perspectives

We discussed the architecture of mini-LED backlit LCD and methods to improve the display performance. First, motion blur can be mitigated by fast-response LC materials and modes as well as low-duty-ratio driving schemes. Second, high dynamic range and nature-like images can be realised by employing backlight units with two-dimensional arrayed mini-LED local dimming zones with optimised zone density. Third, by computing the power consumption to reach the same ambient contrast ratio at fixed display panel size and the view condition, we found that mini-LED backlit LCDs are more suitable for small-pixel applications in comparison with micro-LED/OLED emissive displays.

Regarding applications that can benefit from mini-LED LCD technology, the first category is high dynamic range medium-size displays such as tablets, notebooks, gaming monitors and vehicle panels. These displays need to accommodate both highly bright viewing conditions and dark ambience. The light source – inorganic mini-LED chips – intrinsically exhibits high reliability and long lifetime to support high display brightness. The local dimming structure enhances the contrast ratio and saves power from over-illumination. It is worth noting that another candidate – micro-LED display – offers a better pixel-by-pixel dynamic control and potentially has the highest power efficiency, whereas it takes years to reach the target performance for developing the mass production techniques and building the supply-chain ecosystem. During this time window, mini-LED local dimming LCDs are ready to shine by offering a reasonable power consumption and a quite high dynamic range at an affordable price to average consumers. On the other hand, OLED displays outperform LCDs on small-size applications such as smartphones, smartwatches and virtual reality display panels, as far

as the application does not demand very high brightness and decade-long usage. The thin-film structure of OLED makes its power efficiency less sensitive to pixel size, making an advantage over LCDs and micro-LED emissive displays.

Another opportunity for mini-LED LCD is local dimming LCoS for augmented reality (AR) displays. AR displays require ultrahigh brightness because of two reasons. First, the display content needs to be readable in outdoor environment in bright days. While flat panel displays only need to deal with the ~ 4% ambient reflection, AR displays need to address 100% of the ambient because the displayed image floats directly on the real-world scene. Second, 10 ~ 100 times luminance boost on the display panel is expected to compensate for the 90 ~ 99% optical efficiency loss on the combiner in the mainstream waveguide AR display architecture. It makes local dimming backlight especially beneficial for power saving and dynamic range enhancement.

Improvement areas of mini-LED backlit LCD include thickness and efficiency. In conventional direct-lit backlight designs, an optical thickness after the diffuser is necessary for expanding the light from point sources (the mini-LED chips) to a uniform spatial area (the full panel). To reduce the thickness, Apple's Liquid Retina XDR display puts a distributed Bragg reflector on each mini-LED and encapsulates the LED in a resin waveguide layer, which converts the direct-lit structure to an edge-lit configuration in each local dimming zone to reduce the thickness [26]. For such a structure, it is important to balance the illumination uniformity and the optical efficiency. On the other hand, the optical efficiency and the response time are mainly limited by the LCD panel. Strategies include reducing the absorption loss on polarisers, colour filters and black matrix, and employing appropriate LC modes for high transmittance and fast

response time, which are application dependent. In recent years, mini-LED backlit LCD has proven its premium performance in high-end tablets, laptops and gaming monitors, and is receiving increasing attention for vehicle displays. The widespread application of mini-LED backlight is foreseeable, which gives LCD technology new and long-lasting vitality.

Disclosure statement

No potential conflict of interest was reported by the author(s).

References

[1] Heilmeier GH, Zanoni LA, Barton LA. Dynamic scattering: a new electrooptic effect in certain classes of nematic liquid crystals. Proc IEEE. 1968;56(7):1162–1171. doi: 10.1109/PROC.1968.6513

[2] Schadt M, Helfrich W. Voltage-dependent optical activity of a twisted nematic liquid crystal. Appl Phys Lett. 1971;18(4):127–128. doi: 10.1063/1.1653593

[3] Schiekel MF, Fahrenschon K. Deformation of nematic liquid crystals with vertical orientation in electrical fields. Appl Phys Lett. 1971;19(10):391–393. doi: 10.1063/1.1653743

[4] Soref RA. Transverse field effects in nematic liquid crystals. Appl Phys Lett. 1973;22(4):165–166. doi: 10.1063/1.1654597

[5] Schadt M. Milestone in the history of field-effect liquid crystal displays and materials. Jpn J Appl Phys. 2009;48 (3S2):03B001. doi: 10.1143/JJAP.48.03B001

[6] Takeda A, Kataoka S, Sasaki T, et al. 41.1: a super-high image quality multi-domain vertical alignment LCD by new rubbing-less technology. SID Symp Dig Tech Pap. 1998;29(1):1077–1080. doi: 10.1889/1.1833672

[7] Lee SH, Lee SL, Kim HY. Electro-optic characteristics and switching principle of a nematic liquid crystal cell controlled by fringe-field switching. Appl Phys Lett. 1998;73 (20):2881–2883. doi: 10.1063/1.122617

[8] Tang CW, VanSlyke SA. Organic electroluminescent diodes. Appl Phys Lett. 1987;51(12):913–915. doi: 10.1063/1.98799

[9] Baldo MA, You Y, Shoustikov A, et al. Highly efficient phosphorescent emission from organic electroluminescent devices. Nature. 1998;395:151–154. doi: 10.1038/25954

[10] Lee JH, Chen CH, Lee PH, et al. Blue organic light-emitting diodes: current status, challenges, and future outlook. J Mater Chem C. 2019;7(20):5874–5888. doi: 10.1039/C9TC00204A

[11] Amundson K, Sjodin T. 68.1: invited paper: achieving graytone images in a microencapsulated electrophoretic display. SID Symp Dig Tech Pap. 2006;37(1):1918–1921. doi: 10.1889/1.2433425

[12] Kwak Y, Park J, Park DS. Generating vivid colors on red-green-blue-white electronic-paper display. Appl Opt. 2008 Sept 1;47(25):4491–4500. doi: 10.1364/AO.47.004491

[13] Koch T, Yeo JS, Zhou ZL, et al. Novel flexible reflective color media with electronic inks. J Inf Disp. 2011;12 (1):5–10. doi: 10.1080/15980316.2011.563062

[14] Wong MS, Nakamura S, DenBaars SP. Review—progress in high performance III-nitride micro-light-emitting diodes. ECS J Solid State Sci Technol. 2020;9(1):015012. doi: 10.1149/2.0302001JSS

[15] Jiang HX, Jin SX, Li J, et al. III-nitride blue microdisplays. Appl Phys Lett. 2001;78(9):1303–1305. doi: 10.1063/1.1351521

[16] Lee VW, Twu N, Kymissis I. Micro-LED technologies and applications. Inf Disp. 2016;32(6):16–23. doi: 10.1002/j.2637-496X.2016.tb00949.x

[17] Templier F. GaN-based emissive microdisplays: a very promising technology for compact, ultra-high brightness display systems. J Soc Inf Disp. 2016;24 (11):669–675. doi: 10.1002/jsid.516

[18] Huang Y, Hsiang EL, Deng MY, et al. Mini-LED, micro-LED and OLED displays: present status and future perspectives. Light Sci Appl. 2020;9(1):105. doi: 10.1038/s41377-020-0341-9

[19] Kim DY, Kim MJ, Sung G, et al. Stretchable and reflective displays: materials, technologies and strategies. Nano Converg. 2019;6(1):21. doi: 10.1186/s40580-019-0190-5

[20] Utsumi Y, Takeda S, Kagawa H, et al. 11.2: improved contrast ratio in IPS-Pro LCD TV by using quantitative analysis of depolarized light leakage from component materials. SID Symp Dig Tech Pap. 2008;39(1):129. doi: 10.1889/1.3069379

[21] Chen H, Tan G, Li MC, et al. Depolarization effect in liquid crystal displays. Opt Express. 2017;25(10):11315–11328. doi: 10.1364/OE.25.011315

[22] Seetzen H, Heidrich W, Stuerzlinger W, et al. High dynamic range display systems. ACM Trans Graph. 2004;23(3):760–768. doi: 10.1145/1015706.1015797

[23] Tan G, Huang Y, Li MC, et al. High dynamic range liquid crystal displays with a mini-LED backlight. Opt Express. 2018 Jun 25;26(13):16572–16584. doi: 10.1364/OE.26.016572

[24] Wu T, Sher CW, Lin Y, et al. Mini-LED and micro-LED: promising candidates for the next generation display technology. Appl Sci. 2018;8(9):1557. doi: 10.3390/app8091557

[25] Huang Y, Tan G, Gou F, et al. Prospects and challenges of mini-LED and micro-LED displays. J Soc Inf Disp. 2019;27 (7):387–401. doi: 10.1002/jsid.760

[26] Gu MV, Xu D, Calayir V, et al. Apple liquid retina XDR displays with mini-LEDs. SID Symp Dig Tech Pap. 2023;54(1):788–791. doi: 10.1002/sdtp.16680

[27] Hoffman DM, Stepien NN, Xiong W. The importance of native panel contrast and local dimming density on perceived image quality of high dynamic range displays. J Soc Inf Disp. 2016;24(4):216–228. doi: 10.1002/jsid.416

[28] Chen HW, Zhu RD, He J, et al. Going beyond the limit of an LCD's color gamut. Light Sci Appl. 2017;6(9):e17043. doi: 10.1038/lsa.2017.43

[29] Huang YM, Singh KJ, Liu AC, et al. Advances in quantum-dot-based displays. Nanomaterials. 2020;10 (7):1327. doi: 10.3390/nano10071327

[30] 3M optical systems. Vikuiti dual brightness enhancement film (DBEF) [Internet]. 2008 [cited 2020 Mar 11].

Available from: http://www.opticalfilters.co.uk/includes/downloads/3m/DBEF_E_DS_7516882.pdf

[31] Kurita T. 35.1: moving picture quality improvement for Hold-type AM-LCDs. SID Symp Dig Tech Pap. 2001;32 (1):986–989. doi: 10.1889/1.1832037

[32] Peng F, Chen H, Gou F, et al. Analytical equation for the motion picture response time of display devices. J Appl Phys. 2017;121(2):023108. doi: 10.1063/1.4974006

[33] Daly S, Kunkel T, Sun X, et al. 41.1: distinguished paper: viewer preferences for shadow, diffuse, specular, and emissive luminance limits of high dynamic range displays. SID Symp Dig Tech Pap. 2013;44(1):563–566. doi: 10.1002/j.2168-0159.2013.tb06271.x

[34] Helman JL. I3.4: invited paper: delivering high dynamic range video to consumer devices. SID Symp Dig Tech Pap. 2015;46(1):292–295. doi: 10.1002/sdtp.10469

[35] Society of Motion Picture and Television Engineers. High dynamic range electro-optical transfer function of mastering reference displays. ST 2084:2014. 2014. doi:10.5594/SMPTE.ST2084.2014

[36] Chen H, Tan G, Wu ST. Ambient contrast ratio of LCDs and OLED displays. Opt Express. 2017;25 (26):33643–33656. doi: 10.1364/OE.25.033643

[37] Deng L, Zhang X, Yan Y, et al. Ambient contrast ratio of quantum-dot color-converted micro-LED displays. Results Phys. 2023;48:106462. doi: 10.1016/j.rinp.2023.106462

[38] Huang Y. High-fidelity mini-LED and micro-LED displays. Electron Theses Diss. 2020;61.

[39] Yang DK, Wu ST. Fundamentals of liquid crystal devices. 2nd ed. Chichester (UK): John Wiley & Sons; 2015.

[40] Wu ST. Design of a liquid crystal based tunable electro-optic filter. Appl Opt. 1989;28(1):48–52. doi: 10.1364/AO.28.000048

[41] Huang Y, He Z, Wu ST. Fast-response liquid crystal phase modulators for augmented reality displays. Opt Express. 2017;25(26):32757–32766. doi: 10.1364/OE.25.032757

[42] Lee SH, Kim HY, Park IC, et al. Rubbing-free, vertically aligned nematic liquid crystal display controlled by in-plane field. Appl Phys Lett. 1997;71(19):2851–2853. doi: 10.1063/1.120153

[43] Matsushima T, Okazaki K, Yang Y, et al. 43.2: new fast response time in-plane switching liquid crystal mode. SID Symp Dig Tech Pap. 2015;46(1):648–651. doi: 10.1002/sdtp.10237

[44] Choi TH, Woo JH, Choi Y, et al. Effect of two-dimensional confinement on switching of vertically aligned liquid crystals by an in-plane electric field. Opt Express. 2016;24(18):20993–21000. doi: 10.1364/OE.24.020993

[45] Kikuchi H, Yokota M, Hisakado Y, et al. Polymer-stabilized liquid crystal blue phases. Nat Mater. 2002;1 (1):64–68. doi: 10.1038/nmat712

[46] Yan J, Rao L, Jiao M, et al. Polymer-stabilized optically isotropic liquid crystals for next-generation display and photonics applications. J Mater Chem. 2011;21 (22):7870–7877. doi: 10.1039/c1jm10711a

[47] Hikmet RAM. Electrically induced light scattering from anisotropic gels. J Appl Phys. 1990;68(9):4406–4412. doi: 10.1063/1.346190

[48] Sun J, Wu ST. Recent advances in polymer network liquid crystal spatial light modulators. J Polym Sci Part B. 2013;52(3):183–192. doi: 10.1002/polb.23391

[49] Chen Y, Wu ST. Recent advances on polymer-stabilized blue phase liquid crystal materials and devices. J Appl Polym Sci. 2014;131(13):40556. doi: 10.1002/app.40556

[50] Rao L, Yan J, Wu ST, et al. A large Kerr constant polymer-stabilized blue phase liquid crystal. Appl Phys Lett. 2011;98(8):081109. doi: 10.1063/1.3559614

[51] Wittek M, Tanaka N, Wilkes D, et al. 4.4: new materials for polymer-stabilized blue phase. SID Symp Dig Tech Pap. 2012;43(1):25–28. doi: 10.1002/j.2168-0159.2012.tb05699.x

[52] Haseba Y, Yamamoto SI, Sago K, et al. 22.1: invited paper: low-voltage polymer-stabilized blue-phase liquid crystals. SID Symp Dig Tech Pap. 2013;44(1):254–257. doi: 10.1002/j.2168-0159.2013.tb06193.x

[53] Rao L, Ge Z, Wu ST, et al. Low voltage blue-phase liquid crystal displays. Appl Phys Lett. 2009;95(23):231101. doi: 10.1063/1.3271771

[54] Kim M, Kim MS, Kang BG, et al. Wall-shaped electrodes for reducing the operation voltage of polymer-stabilized blue phase liquid crystal displays. J Phys D Appl Phys. 2009;42 (23):235502. doi: 10.1088/0022-3727/42/23/235502

[55] Huang Y, Chen H, Tan G, et al. Optimized blue-phase liquid crystal for field-sequential-color displays. Opt Mater Express. 2017;7(2):641–650. doi: 10.1364/OME.7.000641

[56] Yamamoto T, Ikenaga M, Yamashita A, et al. 16.2: crystalline OS-LCD using blue-phase liquid crystal having characteristic texture. SID Symp Dig Tech Pap. 2012;43(1):201–204. doi: 10.1002/j.2168-0159.2012.tb05747.x

[57] Masaoka K, Nishida Y. Metric of color-space coverage for wide-gamut displays. Opt Express. 2015;23 (6):7802–7808. doi: 10.1364/OE.23.007802

[58] Zhu R, Luo Z, Chen H, et al. Realizing Rec. 2020 color gamut with quantum dot displays. Opt Express. 2015;23 (18):23680–23693. doi: 10.1364/OE.23.023680

[59] Chen H, He J, Wu ST. Recent advances on quantum-dot-enhanced liquid-crystal displays. IEEE J Sel Top Quantum Electron. 2017;23(5):1–11. doi: 10.1109/JSTQE.2017.2649466

[60] Kim SE, An JY, Hong JJ, et al. How to reduce light leakage and clipping in local-dimming liquid-crystal displays. J Soc Inf Disp. 2009;17(12):1051–1057. doi: 10.1889/JSID17.12.1051

[61] Chen H, Ha TH, Sung JH, et al. Evaluation of LCD local-dimming-backlight system. J Soc Inf Disp. 2010;18 (1):57–65. doi: 10.1889/JSID18.1.57

[62] Tian P, McKendry JJD, Gong Z, et al. Size-dependent efficiency and efficiency droop of blue InGaN micro-light emitting diodes. Appl Phys Lett. 2012;101 (23):231110. doi: 10.1063/1.4769835

[63] Lu MHM, Hack M, Hewitt R, et al. Power consumption and temperature increase in large area active-matrix OLED displays. IEEE/OSA J Disp Technol. 2008;4 (1):47–53. doi: 10.1109/JDT.2007.900924

[64] Zhou L, Xu M, Xia XH, et al. Power consumption model for AMOLED display panel based on 2T-1C pixel circuit. J Disp Technol. 2016;12(10):1064–1069. doi: 10.1109/JDT.2016.2583665

[65] Sadasivan S, Bausemer K, Corliss S, et al. 27-1: invited paper: performance benchmarking of wide color gamut televisions and monitors. SID Symp Dig Tech Pap. 2016;47(1):333–335. doi: 10.1002/sdtp.10672

[66] Ahmed K. 11-2: micro LEDs efficiency targets for displays. SID Symp Dig Tech Pap. 2019;50(1):125–128. doi: 10.1002/sdtp.12871

[67] Jung T, Choi JH, Jang SH, et al. 32-1: invited paper: review of micro-light-emitting-diode technology for micro-display applications. SID Symp Dig Tech Pap. 2019;50(1):442–446. doi: 10.1002/sdtp.12951

[68] Kim KH, Lee S, Moon CK, et al. Phosphorescent dye-based supramolecules for high-efficiency organic light-emitting diodes. Nat Commun. 2014;5(1):5769. doi: 10.1038/ncomms5769

[69] Hosoumi S, Yamaguchi T, Inoue H, et al. 3-4: ultra-wide color gamut OLED display using a deep-red phosphorescent device with high efficiency, long life, thermal stability, and absolute BT.2020 red Chromaticity. SID Symp Dig Tech Pap. 2017;48 (1):13–16. doi: 10.1002/sdtp.11562

[70] Takita Y, Takeda K, Hashimoto N, et al. Highly efficient deep-blue fluorescent dopant for achieving low-power OLED display satisfying BT.2020 chromaticity. J Soc Inf Disp. 2018;26(2):55–63. doi: 10.1002/jsid.634

[71] Sasabe H, Nakanishi H, Watanabe Y, et al. Extremely low operating voltage green phosphorescent organic light-emitting devices. Adv Funct Mater. 2013;23 (44):5550–5555. doi: 10.1002/adfm.201301069